Chemical Shifts in Liquid Water Calculated by Molecular Dynamics Simulations and Shielding Polarizabilities

3 AUTHORS, INCLUDING:

Per-Olof Åstrand
Norwegian University of Science and Techno…
106 PUBLICATIONS   2,885 CITATIONS

SEE PROFILE

Kurt V Mikkelsen
University of Copenhagen
266 PUBLICATIONS   6,573 CITATIONS

SEE PROFILE

Chemical Shifts in Liquid Water Calculated by Molecular Dynamics Simulations and Shielding Polarizabilities

Thomas M. Nymand,[†] **Per-Olof Åstrand,**[*,‡] **and Kurt V. Mikkelsen**[‡]

Department of Chemistry, Aarhus University, DK-8000 Århus C, Denmark, and Chemistry Laboratory III, H. C. Ørsted Institute, University of Copenhagen, DK-2100 København Ø, Denmark

The gas-to-liquid chemical shifts of water have been calculated by combining molecular dynamics simulations and quantum chemically derived shielding polarizabilities. The use of a force field based on intermolecular perturbation theory ensures that the electric fields are adequately modeled. The experimental proton shift and its temperature dependence are reproduced, but the oxygen shift lacks higher order terms such as the linear field-gradient contribution. Shifts arising from the difference in the gas phase and liquid geometries of the water molecule have been estimated and discussed.

I. Introduction

Nuclear magnetic resonance (NMR) measurement of chemical shifts is one of the most sensitive methods for determining the structure of molecules and complexes.[1] For example, the nonequivalence of the chemical shifts in proteins allows the structure to be determined, but the origin of the chemical-shift differences is poorly understood. A common method to estimate this effect is to consider electric-field contributions by using protein electrostatics and atom-type shielding polarizabilities.[2] Furthermore, since the nuclear shielding is an extremely sensitive probe of the charge distribution around an atom, the gas-to-liquid shift is a sensitive measurement of how the surrounding medium affects the molecule.

From a theoretical point of view, both intermolecular interactions and the interaction of a molecule with an external magnetic field may be described by perturbation theory.[3−6] Intermolecular perturbation theory has recently been employed in the NEMO approach for constructing accurate intermolecular potentials suitable for molecular dynamics simulations[7−11] and has also recently been extended to intramolecular interactions between different functional groups in large molecules.[12] The NEMO method together with quantum chemically derived shielding polarizabilities therefore presents a consistent approach for accurately calculating the properties needed for obtaining gas-to-liquid chemical shifts as well as chemical-shift nonequivalences in large molecules from first-principle methods. In this work, we shall focus on the most common solvent by considering the gas-to-liquid shift of water.

It is well-established both experimentally[13−17] and theoretically[18−22] that the nuclear shielding of liquid water is different from that of the water molecule in the gas phase. The measured gas-to-liquid shifts ($\sigma_l - \sigma_g$) are −36 ppm for the oxygen shielding[15] and −4.4 ppm for the proton shielding[13] at room temperature. Since the gas-to-liquid shift of the water molecule gives a description of the hydrogen-bonded network in liquid water, it is of fundamental importance for any theoretical model of liquid water that it is able to account for the gas-to-liquid shift.

II. Theoretical Background

The solvent effect on a nuclear shielding constant is normally partitioned as[4]

$$\sigma_{\text{solvent}} = \sigma_b + \sigma_a + \sigma_E + \sigma_w$$

where σ_b is proportional to the magnetic susceptibility, σ_a arises from the anisotropy of the magnetizability of the solvent molecules close to the molecule of interest, σ_w is due to van der Waals interactions, and σ_E is caused by electrostatic interactions that polarize the charge distribution and alter the molecular geometry.

A way to estimate the electrostatic part of the solvation effect, σ_E, is to put the molecule into a cavity within a dielectric medium and calculate the effect quantum chemically.[20] It is then found that it is crucial to optimize the geometry for each dielectric constant since the effect from geometry distortions is found to be large and may alter the sign of the total electrostatic contribution.[23] σ_a may be included by introducing an explicit solvent shell around the molecule of interest,[21] and σ_w may be estimated by carrying out calculations which include electron correlation and a dispersive coupling to the external medium. Calculations at a correlated level will of course also improve the description of the other terms.

Another way to estimate the electrostatic part of the solvent effect is to expand a component of the shielding tensor, $\sigma_{\alpha\beta}$, as[5,24]

$$\sigma_{E,\alpha\beta} = \sigma'_{\alpha\beta,\gamma}E_\gamma + {}^1\!/_2\sigma''_{\alpha\beta,\gamma,\delta}E_\delta E_\gamma + ... + \sigma'_{\alpha\beta,\gamma\delta}E_{\gamma\delta} + {}^1\!/_2\sigma''_{\alpha\beta,\gamma\delta,\epsilon\sigma}E_{\epsilon\sigma}E_{\gamma\delta} + ... \quad (2)$$

where E_γ denotes a component of the electric field and $E_{\gamma\delta}$ a component of the field gradient, respectively, at the nucleus. The Einstein summation convention is used. The shielding (hyper)polarizabilities ($\sigma'_{\alpha\beta,\gamma}$ and $\sigma''_{\alpha\beta,\gamma,\delta}$) have been calculated for the water molecule[25−29] and the transferability of these types of parameters from one molecule to another has been studied recently.[30,31] The electric field (and its gradient) at the atoms of interest may be obtained from molecular dynamics simulations of liquid water.[32] Note that the effect due to distortions of the geometry is not included here. Instead a statistical contribution appears in this approach since ensemble averages of the electric fields and the field gradients are calculated. In order to obtain accurate electric fields, it is important that the force field adopted in the simulation describes the charge distribution of the molecule. It should be noted that many empirical potentials actually fit the r^{-1}-term to model experimental data and are not intended to reproduce the molecular

---

† Aarhus University.
‡ University of Copenhagen.

4106 *J. Phys. Chem. B, Vol. 101, No. 20, 1997*

Nymand et al.
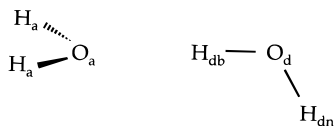
Figure 1. Atomic labels of the water dimer.

dipole and quadrupole moments. Thus they do not contain a proper description of the electrostatics and are therefore not suitable for describing electrostatic effects on molecular properties. As discussed above, a convenient way of calculating potentials that model the electrostatics properly is to use intermolecular perturbation theory,[6] where NEMO is one method based on this idea.[7]

The van der Waals (or dispersion) contribution to the chemical shielding is proportional to the fluctuation potential[33−35]

$$\sigma_w = -B\langle E_0^2 \rangle \tag{3}$$

which is related to the dispersion energy as[36]

$$E_{disp} = -{}^1/_4 \alpha \langle E_0^2 \rangle \tag{4}$$

where $\langle E_0^2 \rangle$ is the fluctuation potential, α is the isotropic polarizability, and B is an isotropic shielding hyperpolarizability. In the NEMO model, the dispersion energy is described with an atomic site London formula,[7]

$$E_{disp}^{Lon} = -\frac{C}{4} \frac{\bar{\omega}^A \bar{\omega}^B}{\bar{\omega}^A + \bar{\omega}^B} \sum_{ij} \alpha_{\alpha\beta}^i \alpha_{\gamma\delta}^j T_{\alpha\gamma}^{ij} T_{\beta\delta}^{ij} \tag{5}$$

where $\alpha_{\alpha\beta}$ is a component of an atomic polarizability tensor,[37−39] $T_{\alpha\beta}^{ij}$ is a component of the so-called interaction tensor $(\nabla_\alpha \nabla_\beta (1/R_{ij}))$, $\bar{\omega}^A$ is an averaged ionization potential of molecule A, and C is a correction factor of 1.89 calibrated from the H_2–H_2 system.[40] The correction factor arises since the uncoupled Hartree–Fock (UCHF) approximation has been used for calculating the distributed polarizabilities and the averaged ionization potential is approximate. In our model of the dispersion energy, the fluctuation potential $\langle E_0^2 \rangle$ is given as

$$\langle E_0^2 \rangle_{\alpha\beta,i} = \sqrt{C} \frac{\bar{\omega}^A \bar{\omega}^B}{\bar{\omega}^A + \bar{\omega}^B} \sum_j \alpha_{\gamma\delta}^j T_{\alpha\gamma}^{ij} T_{\beta\delta}^{ij} \tag{6}$$

where it should be noted that a second rank tensor is obtained at each atom. Here we have assumed that C is only due to a scaling of the local polarizabilities. This is reasonable since it has been found that molecular polarizabilities calculated within the UCHF approximation are about 70−80% of more accurate values obtained in calculations.[41,42] The dispersive contribution to the shift may thus be calculated as

$$\sigma_{w,\alpha\beta} = {}^1/_2 \sigma''_{\alpha\beta,\gamma\delta} \langle E_0^2 \rangle_{\gamma\delta} \tag{7}$$

The expansion considered for the electrostatic and dispersion terms is only correct in the long-range limit; *i.e.* the overlap of the molecular wave functions is neglected. Overlap contributions have been studied for interatomic interactions, and the effects have been found to be significant.[43−47]

The solvent term proportional to the magnetic susceptibility is zero for a spherical sample, but for a cylindrical sample it is given by,[48]

$$\sigma_{b,cyl} = {}^2/_3 \pi \chi_v \tag{8}$$

where χ_v is the volume susceptibility. The effects from the

TABLE 1: Electric Field Shifts (in ppm) of the Water Dimer

	perturbation			finite field[a]	
	1st order	2nd order	total	shielding	shift[b]
O_d	2.88	−0.26	2.62	310.74	1.75
H_{db}	−2.97	0.17	−2.79	28.175	−2.78
H_{dn}	0.33	0.00	0.33	31.273	0.32
O_a	5.24	−0.18	5.06	312.82	3.83
H_a	−0.64	0.01	−0.63	30.332	−0.62

[a] The oxygen basis set has been contracted to [4s3p2d] and the hydrogen basis set to [3s2p]. [b] The monomer shieldings are: $\sigma^O = 308.99$ ppm, $\sigma^H = 30.956$ ppm.

anisotropy of the magnetizability of the nearby molecules on a component of the shielding tensor, σ_a^j, may be obtained from the expression for the magnetic field[4]

$$\mathbf{H} = \mathbf{H}^0 + {}^1/_3 R^{-5}(3r_\alpha r_\beta - R^2 \delta_{\alpha\beta})\xi_{\alpha\beta}^j \mathbf{H}^0 = $$
$$\mathbf{H}^0 + {}^1/_3 T_{\alpha\beta}^{ij} \xi_{\alpha\beta}^j \mathbf{H}^0 \tag{9}$$

where $\xi_{\alpha\beta}^j$ is a component of the molecular magnetizability tensor of molecule j, which also is accessible from quantum chemical calculations,[49] and $\mathbf{H}$ is the magnetic field. The contribution to the shift is thus given by

$$\sigma_a^j = -{}^1/_3 T_{\alpha\beta}^{ij} \xi_{\alpha\beta}^j \tag{10}$$

It is, however, required that R is large compared to the molecular dimension for the model to converge,[4] which is not the case for liquid water. An improvement would be to develop distributed magnetizabilities in line with distributed polarizabilities.

III. Nuclear Shieldings of the Water Dimer

The nuclear shieldings of the water dimer have been studied extensively with *ab initio* methods.[50−54] It is, however, difficult to assess accurate values of the chemical shifts of the water dimer since it is difficult to determine one single accurate structure of the dimer.[55] In this part, the purpose is to investigate if it is possible to reproduce the chemical shifts obtained in a supermolecule calculation on the water dimer at the Hartree–Fock level by only considering

$$\sigma_{E,\alpha\beta} = \sigma'_{\alpha\beta,\gamma} E_\gamma + {}^1/_2 \sigma''_{\alpha\beta,\gamma,\delta} E_\gamma E_\delta \tag{11}$$

a form which was originally adopted by Buckingham for calculating both intramolecular and intermolecular proton shifts.[4,5] We have used the shielding polarizabilities of Rizzo *et al.* (labeled *HF/our geometry* in ref 29), and the electric fields have been calculated with a NEMO potential.[11] The geometry of the water dimer is taken from ref 55 and the atomic labels are given in Figure 1. First we compare with a finite field calculation, where the electric fields of the NEMO potential have been added to the one-electron Hamiltonian. We have used the Dalton program[56] and the atomic natural orbital (ANO) basis sets by Widmark.[57] It is noted in Table 1 that the perturbation expansion and the finite field calculations give similar results and that the perturbation expansion is valid for the size of electric fields present in the water dimer.

The next step is to carry out explicit calculations of the shielding of the water dimer for the same geometry at the Hartree–Fock level. It is noted that the basis set superposition errors (BSSE) may be severe.[52] Instead of correcting for the BSSE with the counterpoise method,[58] we have increased the size of the basis set until it is assumed that the BSSE is small.

Chemical Shifts in Liquid Water

J. Phys. Chem. B, Vol. 101, No. 20, 1997 **4107**

TABLE 2: Chemical Shifts (in ppm) of the Water Dimer at the Hartree−Fock Level

basis set	monomer shieldings		dimer shifts				
	O	H	O_d	H_{db}	H_{dn}	O_a	H_a
ANO[4s3p2d/3s2p]	308.99	30.96	−6.04	−3.38	0.59	−7.08	−0.48
ANO[5s4p3d/4s3p]	330.39	30.80	−0.47	−3.03	0.49	−4.74	−0.52
ANO[5s4p3d2f/4s3p2d]	328.02	30.61	−0.54	−3.05	0.49	−5.27	−0.54
ANO[6s5p4d/5s4p]	326.78	30.77	−0.26	−3.05	0.50	−7.38	−0.54
ANO[6s5p4d3f/5s4p3d]	327.97	30.56	−0.97	−3.04	0.50	−7.66	−0.53
ANO uncontracted	327.78	30.57	−0.58	−3.04	0.51	−7.38	−0.53

TABLE 3: Electric Field Components (in 10^{-3} Atomic Units) at the Nuclei of the Water Molecule

T, K	$\langle E_z^O \rangle$	$\langle E_{\parallel}^H \rangle^a$	$\langle E_{\perp}^H \rangle^a$
269	52.7	53.8	0.0
300	49.6	50.3	0.0
338	45.0	45.2	0.0
448	35.1	34.5	0.0

^{a} $\parallel$ and $\perp$ denote parallel and perpendicular to the O−H bond, respectively.

The counterpoise method has, however, been adopted for the uncontracted ANO basis set, and it is found that the BSSE is of the order of 0.001 ppm for this basis set. The results for different contractions of the ANO basis set are given in Table 2.

If the perturbation and finite field approaches in Table 1 are compared with the dimer calculations in Table 2, it is noted that the proton shifts are modeled within a few tenths of a ppm. The oxygen shieldings are, on the other hand, not even qualitatively modeled with an electric-field approach. The oxygen shifts have the wrong sign and are in error by about 5−10 ppm. Consequently, other terms such as field-gradient contributions, effects from the magnetizability anisotropy of the other molecule and possibly overlap effects[59] are important for the oxygen shift. It is therefore not expected that we will be able to mimic the oxygen gas-to-liquid shift for water with this model, and we will instead focus on the proton shift.

IV. Molecular Dynamics Simulations

The Molsim program[60] with the extensions to a NEMO potential with atomic dipole moments and atomic polarizability tensors[11] has been used in the molecular dynamics simulations. The simulated system consists of 216 water molecules enclosed in a cubic box. In the calculation of the forces, periodic boundary conditions have been adopted with a spherical cutoff of 8.5 Å. The induced dipole moments have been calculated by a first-order predictor method, but a full iterative solution has been carried out every fifth time step in order to avoid drifting.[61] The canonical ensemble was employed by scaling the velocities to the appropriate temperature.[62] The equations of motion of the rigid molecules were integrated by using quaternions[63] and the velocity Verlet algorithm.[64] We have carried out simulations of 110 ps (including 10 ps of equilibration) at four different temperatures, 269, 300, 338, and 448 K, at experimental densities.

The z-axis is chosen as the C_2-axis, and the water molecule is placed in the xz-plane. Properties of the hydrogen atom situated in $(+x,0,+z)$ are presented. The ensemble averages of the components of the electric field at each type of atom are calculated and presented in Table 3. For symmetry reasons it is only the field along the dipole moment axis that contributes to the electric field at the oxygen atom, but it is interesting to note that only the field along the O−H bond contributes to the total field at the hydrogen atom. It is furthermore noted that
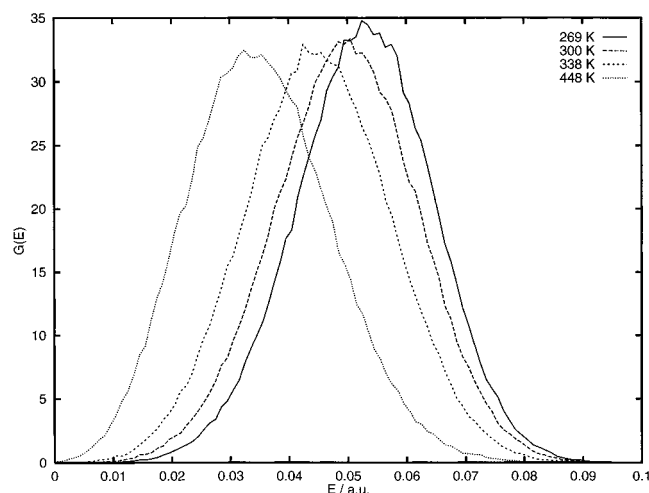
Figure 2. Electric field distributions at the oxygen atom.
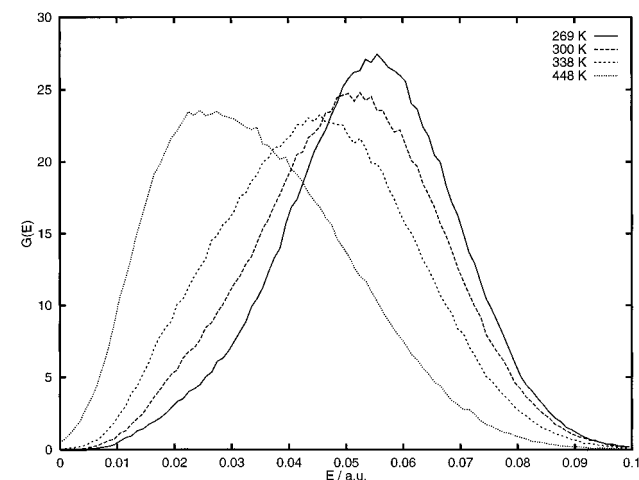
Figure 3. Electric field distributions at the hydrogen atom.

TABLE 4: Gaussian Distributions, $G(E) = ae^{-(1/2)((E-c)^2/b^2)}$, of the Electric Field at the Oxygen Atom (in Atomic Units)

T, K	a	b	c
269	34.37	0.011 59	0.053 04
300	32.92	0.012 12	0.049 81
338	32.34	0.012 37	0.044 86
448	32.66	0.012 27	0.034 42

TABLE 5: Gaussian Distributions, $G(E) = ae^{-(1/2)((E-c)^2/b^2)}$, of the Electric Field at the Hydrogen Atom (in Atomic Units)

T, K	a	b	c
269	26.72	0.014 84	0.054 57
300	24.40	0.016 44	0.050 76
338	23.24	0.017 44	0.044 74
448	24.05	0.016 73	0.032 02

the electric field decreases as the temperature increases. These field distributions are presented in Figures 2 and 3 and each of them is fitted to a Gaussian function (Tables 4 and 5). As seen from Figure 4 the field distributions are almost perfectly described with Gaussian functions, and it is only the field at the hydrogen atom at 448 K (Figure 5) that is not modeled with a Gaussian function. It is actually a nice feature of liquid water that the electric fields may be described with only two Gaussian functions.

It is also of interest to calculate $\langle E_\alpha E_\beta \rangle$ since it gives the second term in eq 2. (See Tables 6 and 7). As expected, the most important components by far are $\langle E_z E_z \rangle$ for the oxygen atom and $\langle E_{\parallel} E_{\parallel} \rangle$ for the hydrogen atom, and it is noted that they also decrease with increasing temperature.
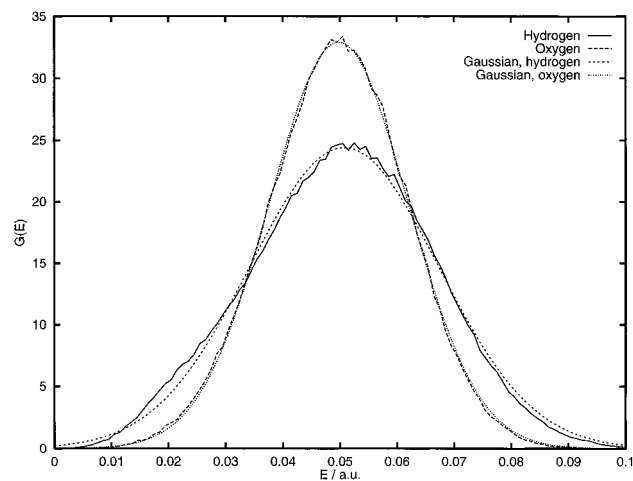
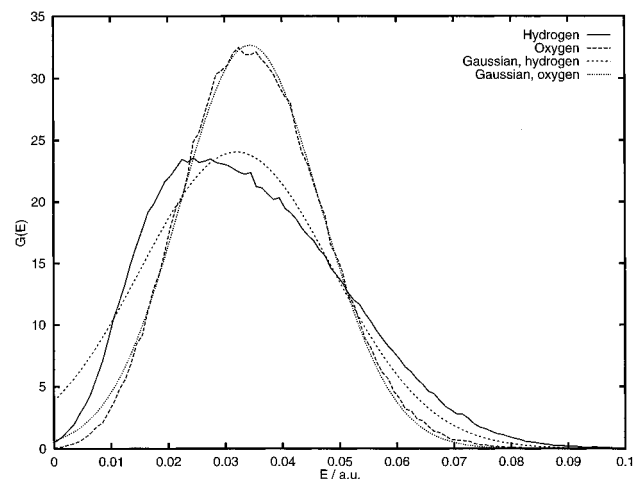**Figure 4.** Gaussian distributions of the electric fields at 300 K.

Figure 5. Gaussian distributions of the electric fields at 448 K.

TABLE 6: The Mean Square of the Electric Field Components (in 10^{-3} Atomic Units) at the Oxygen Atom

	269 K	300 K	338 K	448 K
$\langle E_x E_x \rangle$	0.10	0.10	0.10	0.09
$\langle E_y E_y \rangle$	0.22	0.23	0.22	0.19
$\langle E_z E_z \rangle$	2.92	2.61	2.17	1.38

TABLE 7: The Mean Square of the Electric Field Components (in 10^{-3} Atomic Units) at the Hydrogen Atom

	269 K	300 K	338 K	448 K
$\langle E_\| E_\| \rangle$	3.02	2.67	2.19	1.32
$\langle E_\| E_\perp \rangle$	0.00	0.00	0.00	0.00
$\langle E_\perp E_\perp \rangle$	0.04	0.04	0.04	0.04
$\langle E_y E_y \rangle$	0.07	0.08	0.08	0.08

V. Solvent Effects on Nuclear Shieldings

We have used the shielding polarizabilities obtained by Rizzo *et al.* with their largest CAS space (labeled CAS B).[29] The authors state that these values are converged with respect neither to basis nor to electron correlation, but we think that these values are the best available at the present time. It should also be noted that the shielding polarizabilities are strongly dependent on the geometry.[29]

The effect on the nuclear shielding from a uniform electric field is calculated from the first two terms in eq 2

$$\langle \sigma_{E,\alpha\beta} \rangle = \sigma'_{\alpha\beta,\gamma} \langle E_\gamma \rangle + {}^1\!/_2 \sigma''_{\alpha\beta,\gamma,\delta} \langle E_\gamma E_\delta \rangle \qquad (12)$$

The results as a function of temperature are given in Tables 8

TABLE 8: Electric Field Effects on Oxygen Shielding (in ppm)

T, K	1st order	2nd order	total
269	17.75	−4.02	13.73
300	16.71	−3.60	13.11
338	15.14	−3.01	12.13
448	11.83	−1.93	9.90

TABLE 9: Electric Field Effects on Proton Shielding (in ppm)

T, K	1st order	2nd order	total
269	−4.35	0.26	−4.09
300	−4.06	0.23	−3.83
338	−3.64	0.18	−3.44
448	−2.76	0.10	−2.66

TABLE 10: van der Waals Contributions to the Gas-to-Liquid Shifts of Water (in ppm)

	oxygen		hydrogen	
T, K	tensor	isotropic	tensor	isotropic
269	−8.89	−5.73	0.03	−0.40
300	−8.76	−5.71	−0.02	−0.38
338	−8.35	−5.01	−0.07	−0.35
448	−7.07	−3.99	−0.16	−0.28

TABLE 11: Solvent Effects to Nuclear Shielding (in ppm)

	oxygen		hydrogen	
T, K	calc	exptl[a]	calc	exptl[b]
269	4.84		−4.06	−4.70
300	4.34	−36	−3.86	−4.35
338	3.78		−3.53	−4.02
448	2.83	−27	−2.82	

[a] See ref 15. [b] See ref 13.

and 9. The first-order term of the oxygen shift is positive and relatively large compared to the second-order term which is negative. The total electric field contribution is thus positive and changes from about 14 ppm at 269 K to about 10 ppm at 448 K. On the other hand, the first-order contribution is negative for the proton shielding whereas the second-order contribution is positive. The total shift from the electric field changes from −4 ppm at 269 K to about −2.5 ppm at 448 K.

We have calculated the dispersive part, σ_w, both with the tensor form in eq 7 and with the isotropic form in eq 3. As noted from Table 10, we obtain significantly different results with these two approaches. For the oxygen shift, it is noted that the isotropic form gives a less negative shift than the tensor form, and the difference is about 3 ppm. The temperature shift, though, is nearly the same for the isotropic form and the tensor form. For the proton shielding, the tensor form gives an almost negligable shift whereas the isotropic term gives a somewhat larger negative contribution. It is concluded that it is important to use a tensor form, but, on the other hand, the accuracy of the local polarizability tensors will then be crucial for obtaining correct results.

The bulk susceptibility term, σ_b, has been calculated to be −1.5 ppm for all temperatures. The proton shift experiments have, however, already been corrected for the shape of the sample,[13] whereas the geometry of the sample was not known in the oxygen shift experiment.[15]

The total solvent effect is compared with experimental data in Table 11. It is found that the proton shielding is in good agreement with experimental data[13] and previous theoretical work.[18] The temperature dependence is properly described, and it is noted that the calculated values are consistently about 0.5 ppm too large. As expected from the calculations on the water

Chemical Shifts in Liquid Water

J. Phys. Chem. B, Vol. 101, No. 20, 1997 **4109**

TABLE 12: Geometrical Effects to Gas-to-Liquid Shifts

	$R_{O,H}$, Å	$\angle_{HOH}$, deg	σ^O	σ^H
gas phase	0.941	106.5	336.3	31.19
liquid phase[a]	0.961	114.0	326.8	29.79
liquid phase[b]	0.951	110.	331.5	30.50

[a] The geometry is taken from the central molecule in a pentamer that has been geometry-optimized within a dielectric medium. For more details see ref 21. [b] The geometry is taken from a combined quantum chemical calculation and Monte Carlo simulation. For more details see ref 65.

dimer, the gas-to-liquid shift of the oxygen atom is not accurately modeled. We find the shift to be in the range 2.8−4.8 ppm whereas the only experimental value predicts a shift of −36 ppm at room temperature.[15]

VI. Geometrical Effects on Gas-to-Liquid Shifts

The difference in the geometry of the water molecule in the gas phase and the liquid phase has not been considered so far in this work, but it obviously contributes to the gas-to-liquid shift. In this work, we will only estimate the geometrical effects by calculating the Hartree−Fock gas phase shieldings for three different geometries: a gas phase and two liquid phase geometries.[21,65] Since the two liquid phase geometries are rather different from each other (see Table 12) the shifts arising from only changing the geometry also deviate from each other. The geometrical effect on the oxygen shift is substantial (−10 and −5 ppm, respectively), which means that geometrical distortions have to be considered in detail for modeling the total oxygen gas-to-liquid shift. For the proton shift, the effects are −1.4 and −0.7 ppm, respectively, which may explain the difference with respect to the experimental gas-to-liquid shift in Table 11. These results for the intramolecular contribution are in line with recent density functional theory calculations on water clusters, where the structures of the clusters have been selected from molecular dynamics simulations with different nonrigid potentials.[22]

VII. Discussion and Conclusions

In this work, we have used a consistent approach for calculating gas-to-liquid chemical shifts of water which is based on quantum chemical perturbation theory. Both the intermolecular potential and the magnetic properties have been calculated by employing *ab initio* methods, and thus the approach involves no empirical information. This is important for understanding which contributions are important and for the predictive capacity of the method.

The proton shift and its temperature dependence are well-described with the approach employed here, whereas the oxygen shift has not been modeled in a satisfying way. It therefore remains to be investigated whether field-gradient or magnetizability anisotropy terms are important for the oxygen shielding. It is, however, not expected that σ_a will be important for water since the magnetizability of ice is isotropic.[66] On the other hand, field-gradient terms are expected to be large for the oxygen shielding whereas they are probably negligible for proton shielding since the electrons at the hydrogen atom are mainly of s-character. It has been demonstrated that the linear field-gradient term is substantial for carbon shieldings,[24] but to our knowledge no rigorous and accurate approach for calculating the field-gradient derivative of nuclear shieldings exists at the present.

It is furthermore noticed that changes in the molecular geometry due to the surrounding environment are important for the chemical shift, and this term is only approximately estimated

here. Further investigations will require a nonrigid and polarizable water potential and consequently also geometry derivatives of shieldings and shielding polarizabilities. It is also possible that the zero-point vibrational contributions are substantially different in the liquid and in the gas phase, which may be deduced from the different potential surfaces of the water molecule in the liquid and the gas phase[65] and the substantial rovibrational contributions to the shieldings of the water molecule.[67]

An alternative to calculate gas-to-liquid shifts is to carry out a molecular dynamics simulation, pick a set of cluster configurations from this simulation, and then calculate the shieldings quantum chemically.[19,22] It is noted that this procedure gives results for the oxygen gas-to-liquid shifts in the range −47 to −20 ppm for different empirical potentials,[19,22] which indicates how sensitive the oxygen shift is to the intermolecular potential. It is furthermore noted that the proton shieldings calculated with the supermolecule approach[19,22] are in error of about 30% compared to those from the experiment. The supermolecule procedure requires, however, considerably more computer time than the approach adopted here since the shieldings have to be calculated for a set of clusters at each temperature. In a study of the concentration dependence of a property, it would be necessary to include all possible solvent−solute and solute−solute interactions. In that case the supermolecule approach will become far too expensive.

The approach adopted here is, however, straightforward to generalize to both solutions and conformational shifts in large molecules, since the calculation of molecular properties in solution has been partioned into two parts:

(a) Quantum chemical calculations of molecular properties such as shielding polarizabilities for the unperturbed molecule. The properties have to be calculated *once* for each molecule.

(b) Statistical mechanical simulations for calculating the ensemble average of the size of the perturbation, *e.g.* electric field or geometry distortion. The simulation has to be repeated for each temperature (or concentration), but the results may then be used for the calculation of the solvent effects on *any* molecular property.

The accuracy may thus be increased for each part separately in a step-by-step procedure.

References and Notes

(1) Tossell, J. A.; Ed. *Nuclear magnetic shieldings and molecular structure*; NATO ASI Series C, Vol. 386; Kluwer: Dordrecht, The Netherlands, 1993.

(2) Augspurger, J.; Pearson, J. G.; Oldfield, E.; Dykstra, C. E.; Park, K. D.; Schwartz, D. *J. Magn. Res.* **1992**, *100*, 342−357.

(3) Stephen, M. J. *Mol. Phys.* **1958**, *1*, 223−232.

(4) Buckingham, A. D.; Schaefer, T.; Schneider, W. G. *J. Chem. Phys.* **1960**, *32*, 1227−1233.

(5) Buckingham, A. D. *Can. J. Chem.* **1960**, *38*, 300−307.

(6) Buckingham, A. D. *Adv. Chem. Phys.* **1967**, *12*, 107.

(7) Wallqvist, A.; Karlström, G. *Chem. Scr.* **1989**, *29A*, 131−137.

(8) Åstrand, P.-O.; Wallqvist, A.; Karlström, G.; Linse, P. *J. Chem. Phys.* **1991**, *95*, 6395−6396.

(9) Åstrand, P.-O.; Wallqvist, A.; Karlström, G. *J. Chem. Phys.* **1994**, *100*, 1262−1273.

(10) Åstrand, P.-O.; Wallqvist, A.; Karlström, G. *J. Phys. Chem.* **1994**, *98*, 8224−8233.

(11) Åstrand, P.-O.; Linse, P.; Karlström, G. *Chem. Phys.* **1995**, *191*, 195−202.

(12) Engkvist, O.; Åstrand, P.-O.; Karlström, G. *J. Phys. Chem.* **1996**, *100*, 6950−6957.

(13) Hindman, J. C. *J. Chem. Phys.* **1966**, *44*, 4582−4592.

(14) Luz, Z.; Yagil, G. *J. Phys. Chem.* **1966**, *70*, 554−561.

4110 *J. Phys. Chem. B, Vol. 101, No. 20, 1997*

Nymand et al.

(15) Florin, A. E.; Alei, M., Jr. *J. Chem. Phys.* **1967**, *47*, 4269−4269.

(16) Raynes, W. T. *Mol. Phys.* **1983**, *49*, 443−447.

(17) Wasylishen, R. E.; Mooibroek, S.; Macdonald, J. B. *J. Chem. Phys.* **1984**, *81*, 1057−1059.

(18) Svishchev, I. M.; Kusalik, P. G. *J. Am. Chem. Soc.* **1993**, *115*, 8270−8274.

(19) Chesnut, D. B.; Rusiloski, B. E. *J. Mol. Struct.* **1994**, *314*, 19−30.

(20) Mikkelsen, K. V.; Jørgensen, P.; Ruud, K.; Helgaker, T. *J. Chem. Phys.* **1997**, *106*, 1170.

(21) Mikkelsen, K. V.; Ruud, K.; Helgaker, T. *Chem. Phys. Lett.* **1996**, *253*, 443−447.

(22) Malkin, V. G.; Malkina, O. L.; Steinebrunner, G.; Huber, H. *Chem. Eur. J.* **1996**, *2*, 452.

(23) Åstrand, P.-O.; Mikkelsen, K. V.; Ruud, K.; Helgaker, T. *J. Phys. Chem.* **1996**, *100*, 19771−19782.

(24) Batchelor, J. G. *J. Am. Chem. Soc.* **1975**, *97*, 3410−3415.

(25) Augspurger, J. D.; Dykstra, C. E. *J. Phys. Chem.* **1991**, *95*, 9230.

(26) Grayson, M.; Raynes, W. T. *Chem. Phys. Lett.* **1993**, *214*, 473.

(27) Grayson, M.; Raynes, W. T. *Chem. Phys. Lett.* **1994**, *218*, 270.

(28) Grayson, M.; Raynes, W. T. *Chem. Phys. Lett.* **1994**, *224*, 602.

(29) Rizzo, A.; Helgaker, T.; Ruud, K.; Barszczewicz, A.; Jaszuński, M.; P. Jørgensen, *J. Chem. Phys.* **1995**, *102*, 8953−8966.

(30) Grayson, M.; Raynes, W. T. *Mol. Phys.* **1994**, *81*, 533−545.

(31) Grayson, M.; Raynes, W. T. *Magn. Reson. Chem.* **1995**, *33*, 138−143.

(32) Wallqvist, A.; Ahlström, P.; Karlström, G. *J. Phys. Chem.* **1990**, *94*, 1649−1656. Erratum in *J. Phys. Chem.* **1991** *95*, 4922.

(33) Raynes, W. T.; Buckingham, A. D.; Bernstein, H. J. *J. Chem. Phys.* **1962**, *36*, 3481.

(34) Kromhout, R. A.; Linder., B. *J. Magn. Res.* **1969**, *1*, 450−463.

(35) Homer, J.; Mohammadi, M. S. *J. Chem. Soc., Faraday Trans 1* **1988**, *84*, 2959−2966.

(36) London, F. *Trans. Faraday Soc.* **1937**, *33*, 8.

(37) Karlström, G. *Theor. Chim. Acta* **1982**, *60*, 535.

(38) Stone, A. J. *Mol. Phys.* **1985**, *56*, 1065−1082.

(39) Ángyán, J. G.; Jansen, G.; Loos, M.; Hättig, C.; Hess, B. A. *Chem. Phys. Lett.* **1994**, *219*, 267−273.

(40) Karlström, G. *Theor. Chim. Acta* **1980**, *55*, 233−241.

(41) Åstrand, P.-O.; Karlström, G. *Mol. Phys.* **1992**, *77*, 143.

(42) Sanchez de Merás, A. M.; Jensen, H. J. Aa.; Jørgensen, P.; Olsen, J. *Chem. Phys. Lett.* **1991**, *186*, 379−385.

(43) Jameson, C. J.; de Dios, A. C. *J. Chem. Phys.* **1992**, *97*, 417−434.

(44) Jameson, C. J.; de Dios, A. C. *J. Chem. Phys.* **1993**, *98*, 2208−2217.

(45) Jameson, C. J.; Lim, H.-M. *J. Chem. Phys.* **1995**, *103*, 3885−3894.

(46) Freitag, A.; van Wüllen, Ch.; Staemmler, V. *Chem. Phys.* **1995**, *192*, 267−280.

(47) Barszczewicz, A.; Jaszuński, M.; Helgaker, T.; Ruud, K. *Chem. Phys. Lett.* **1996**, *250*, 1−8.

(48) Dickinson, W. C. *Phys. Rev.* **1951**, *81*, 717.

(49) Ruud, K.; Helgaker, T.; Bak, K. L.; Jørgensen, P.; Jensen, H. J. Aa. *J. Chem. Phys.* **1993**, *99*, 3847−3859.

(50) Ditchfield, R. *J. Chem. Phys.* **1976**, *65*, 3123.

(51) Höller, R.; Lischka, H. *Chem. Phys. Lett.* **1981**, *84*, 94.

(52) Ferchiou, S.; Giessner-Prette, C. *Chem. Phys. Lett.* **1983**, *103*, 156.

(53) Hinton, J. F.; Bennet, D. C. *Chem. Phys. Lett.* **1985**, *116*, 292.

(54) Chesnut, D. B.; Rusiloski, B. E. *J. Phys. Chem.* **1993**, *97*, 2839−2845.

(55) Åstrand, P.-O.; Karlström, G.; Engdahl, A.; Nelander, B. *J. Chem. Phys.* **1995**, *102*, 3534.

(56) Helgaker, T.; Jensen, H. J. Aa.; Jørgensen, P.; Olsen, J.; Ågren, H.; Andersen, T.; Bak, K. L.; Bakken, V.; Christiansen, O.; Dahle, P.; Dolskov, E. K.; Enevoldsen, T.; Fernandez, B.; Heiberg, H.; Hettema, H.; Jonsson, D.; Kirpekar, S.; Kobayashi, R.; Koch, H.; Mikkelsen, K. V.; Norman, P.; Packer, M. J.; Ruud, K.; Saue, T.; Taylor, P. R.; Vahtras, O. Dalton, an ab initio electronic structure program.

(57) Widmark, P.-O.; Malmqvist, P.-Å.; Roos, B. O. *Theor. Chim. Acta* **1990**, *77*, 291.

(58) Boys, S. F.; Bernardi, F. *Mol. Phys.* **1970**, *19*, 553.

(59) Buckingham, A. D.; Lawley, K. P. *Mol. Phys.* **1960**, *3*, 219−222.

(60) Linse, P.; Wallqvist, A. MOLSIM 1.2. Lund University, Sweden, 1991.

(61) Ahlström, P.; Wallqvist, A.; Engström, S.; Jönsson, B. *Mol. Phys.* **1989**, *68*, 563−581.

(62) Berendsen, H. J. C.; Postma, J. P. M.; van Gunsteren, W. F.; DiNola, A.; J. R. Haak, *J. Chem. Phys.* **1984**, *81*, 3684−3690.

(63) Allen, M. P.; Tildesley, D. S. *Computer Simulations of Liquids*; Clarendon: Oxford, 1987.

(64) Swope, W. C.; Andersen, H. C.; Berens, P. H.; Wilson, K. R. *J. Chem. Phys.* **1982**, *76*, 637−649.

(65) Moriarty, N. W.; Karlström, G.; Geometry optimisation of a water molecule in water. A combined quantum chemical and statistical mechanical treatment. *J. Chem. Phys.*, in press.

(66) Lonsdale, K. *Nature* **1949**, *164*, 149.

(67) Fowler, P. W.; Raynes, W. T. *Mol. Phys.* **1981**, *43*, 65−82.